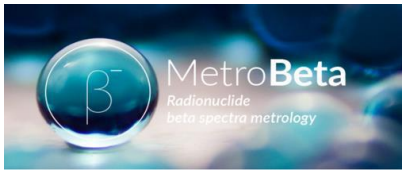

EMPIR
EURAMET
The EMPIR initiative is co-funded by the European Union's Horizon 2020 research and innovation programme and the EMPIR Participating States

Deliverable 8

Grant Agreement number	15SIB10	
Project short name	MetroBeta	
Deliverable title	Comparison between beta spectra measured by means of metallic magnetic calorimeters and obtained by theoretical calculation	
Lead partner	CEA	
Due and actual dates	May 2019	August 2019

TABLE OF CONTENTS

1 Introduction

The two first workpackages of the project are dedicated to the theoretical calculation of the shapes of beta spectra and to their measurement with high energy resolution by means of metallic magnetic calorimeters.

In terms of theoretical calculation, the two main aims were to improve the precision of the calculation beyond the current state of the art, and to assess the theoretical uncertainties. Apart from the three-body process that generates a continuous energy spectrum for the emitted electrons, the shape of a beta spectrum is also influenced by the nature of the transition that can be "allowed" or "forbidden", depending on the structure of the nuclei involved, and by various atomic effects. Therefore the calculations have to take into account the influence of both the atomic and nuclear structure. The main difficulty is to unify the theoretical approaches from both nuclear and atomic physics communities. Another particular challenge from a metrological perspective was the evaluation of the uncertainties of the calculations due to the theoretical models.

First measurements of beta spectra by means of metallic magnetic calorimeters had been undertaken prior to the Metrobeta project, but with MMC detectors that were not optimized for beta spectra measurements, and without any systematic work on radionuclide source preparation. Both of these aspects have been addressed with the project. In particular the physical and chemical properties of the sources have a crucial importance for the quality of the measured spectra.

2 Work description

The theoretical calculation of beta spectra, corresponding to WP1 of the project, has been conducted in collaboration between CEA and UMCS. The theoretical and computational approaches are reported in deliverable D1.

The beta spectra of for nuclides, ^{14}C, ^{151}Sm, ^{99}Tc and ^{36}Cl, have been measured by means of metallic magnetic calorimeters (MMCs, [1,2]) in WP2, both at CEA and PTB. The development of an optimized beta spectrometer based on MMCs for these measurements is reported in deliverable D5. The following paragraphs describe the work concerning the measurements as such, starting from the source preparation and source-absorber integration, and compare the measured spectra with those obtained by theoretical calculation in WP1.

2.1. Source preparation techniques

The source preparation is crucial for the precise measurement of beta spectra with MMCs. The radioactive material must be completely embedded into an absorber consisting of an appropriate material to ensure that every beta particle is detected, and the entire energy is deposited and thermalized, i. e. transformed to heat. Within the framework of this project, the radioactive material was deposited by two different methods, electrodeposition as well as drop deposition, either directly onto the absorber material or onto a separate source carrier foil. To enclose the sources inside the absorber and realize a 4π geometry, in the first case a second foil of absorber material was placed on top of the first foil with the source, in the second case the source carrier foil was sandwiched between bottom and top absorber foils. Each stack of foils was then bonded together by diffusion welding. Temperature, pressure and processing time were varied to fabricate the 4π source/absorber assemblies. The parameters to obtain reliable enclosure were found to depend strongly on the absorber material as well as on the radionuclide and the chemical composition of the source material.

The best source preparation approach - besides implanting the radionuclide directly into the absorber material - is a metallic layer formed by electrodeposition, as long as this is possible for the considered element. In many cases, an oxide/hydroxide layer will form during electrodeposition. This can still be a good quality source consisting in a very thin, homogenous layer. In the past, some experience has been gained with electrodeposition of beta emitters for MMC-based measurements, forming both metal (^{63}Ni) and oxide/hydroxide (^{241}Pu) layers [3]. Within this project, a ^{151}Sm source was

electrodeposited on a silver foil, forming a Sm oxide/hydroxide layer. Also ^{99}Tc was electrodeposited; the deposit is barely visible but, according to the adopted electrodeposition procedure, should be metallic technetium.

Where electrodeposition is not possible, as in the case of ^{14}C or ^{36}Cl, drop-deposited sources were produced. Typical radionuclide solutions contain certain salt loads, which means that drop deposition often leads to the formation of large (of order of micrometers) salt crystals. Previous studies have revealed that salt crystals can cause considerable spectrum distortion due to incomplete thermalization [4]. One approach to avoid the formation of large salt crystals is to decrease the individual drop size to a few picolitres, and to deposit a number of droplets corresponding to the required activity in a 2D-array pattern. Commercial micro-dispensing systems can deposit single droplet volumes of less than 50 pl in combination with a placement accuracy of better than 20 µm. With the help of an automated micro-dispensing system different radionuclide solutions (^{36}Cl, ^{99}Tc, and ^{14}C) were deposited onto gold foils. Milling techniques were used to format gold foils into an array of absorber elements with lateral dimensions of about 0.7 mm and 1.6 mm. Fig. 1a shows an absorber array after the radioactive solution was dried. Here, volumes of 100 nl (left half) and 50 nl (right half) of a ^{99}Tc solution were deposited in the middle of each marked absorber. The fact that the deposit is not visible indicates the absence of large crystallizations. Checking the activity by visual inspection is hence not possible but based on the results of an autoradiographic image, see Fig. 1b, the positions and the different activities of the deposited material were confirmed. The quality of a drop-deposited source, prepared with a micro-dispensing system, can be demonstrated by comparing its measured spectrum with that of an electroplated source.

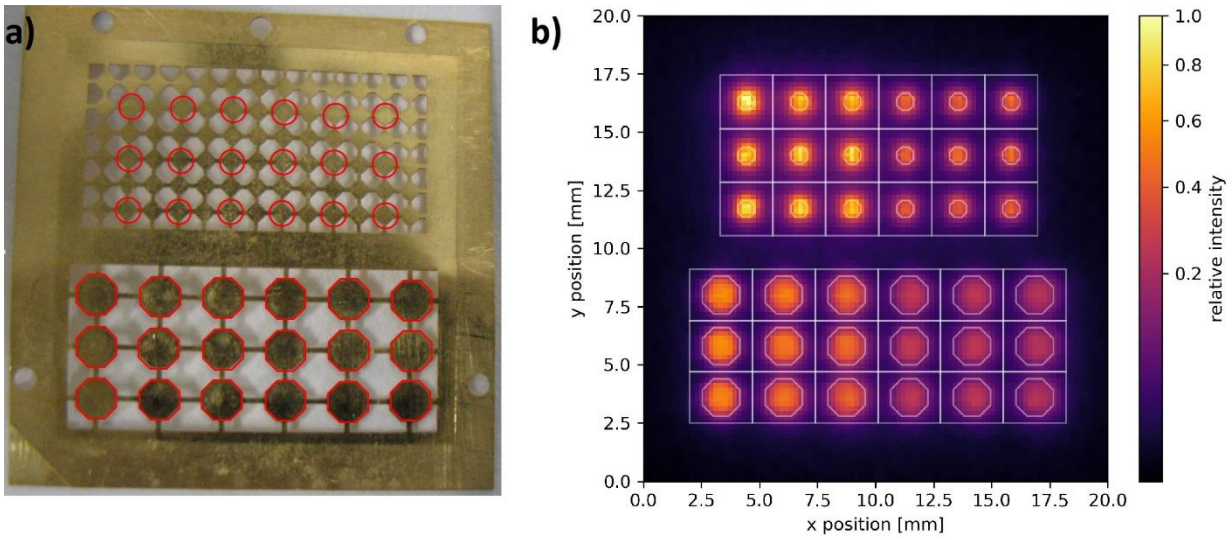

Figure 1: a) Photograph of an array of pre-fabricated gold absorber foils with ^{99}Tc sources deposited by a microdrop dispenser system in the middle of the marked absorbers. b) Autoradiographic image of the same array. Two different activities, 5 Bq / 2.5 Bq, have been deposited on each marked absorber in the left / right half of the array. The activity is well centered on each absorber.

Fine dispersion of the source material in the absorber metal will also improve the source quality compared to a conventional drop-deposited source. One technique resulting in fine dispersion consists in alternate folding and laminating of the foil with the source deposit. This breaks the source crystals into tens of nanometer small particles that are embedded in the metal foil [5]. Since, after this mechanical processing, the activity is dispersed in the entire foil volume, this source foil must then be sandwiched between two metal foils of the required thickness. This technique was applied to the electrodeposited ^{151}Sm source, because its layer was blackish and was considered not to be ideally thin. Another technique resulting in fine dispersion consists in the absorption of radionuclide solutions into nano-porous metal samples. In the context of *Q* spectroscopy of alpha emitters [6],

deposition of actinide solutions into gold nanofoam [7], constraining the crystals to the pore size of tens of nanometers, is also being studied. The gold nanofoam has been prepared by de-alloying a gold-silver alloy with phosphoric acid. The pore size can be controlled via the concentration and the temperature of the etchant and the etching time.

Novel bilayer absorbers are being developed, in order to measure the beta spectrum of ^{36}Cl (Q = 709.53 keV) which suffers from distortion due to bremsstrahlung escape when pure gold absorbers are employed. The distortions are reduced by embedding the radionuclide into 2 x 150 µm copper foils (Z = 29) and adding additional 2 x 200 µm gold foils (Z = 79) around the copper. While the copper layers lead to less bremsstrahlung generation and reduce the energy of the emitted beta particles, the high stopping power of the surrounding gold layers fully stops the electrons while keeping the overall absorber dimensions and the related heat capacity small. Preparing this kind of absorbers requires several steps of diffusion welding in an oxygen-free oven to avoid the oxidation of the copper.

2.2. Beta spectrum measurements

So far, three beta spectra have been measured using MMCs within the MetroBeta project; as already mentioned, the more challenging measurement of the spectrum of ^{36}Cl is under preparation.

^{14}C

The spectrum of ^{14}C has been measured using a source prepared by conventional drop deposition, but from a carrier-free, high specific activity solution. After drying, the deposit was invisible, even under an optical microscope, so the source can be considered to be of high quality. It was deposited on a 25 µm thick gold foil, thick enough to stop all beta particles up to the end point of the spectrum (156.5 keV). Since the ^{14}C atoms are bound in a volatile organic compound, diffusion welding is not a viable option for source enclosure. The foil with the source was just folded over and slightly pressed. Gold is highly ductile and keeps its shape once folded; no beta electrons can escape from being absorbed in the gold absorber. Gold is a good thermal conductor at very low temperature, so the thermal contact between the two halves of the absorber through the bending is sufficient. The absorber (Au, 1 mm^2 × (2 × 25 µm)) was placed on an MMC chip whose size best matches its heat capacity (C_{abs} = 67 pJ/K at 20 mK). The experimental conditions during the spectrum measurement were far from optimal. During the cooling phase, the glue layer fixing the MMC chip to its holder broke, the chip was then only suspended by the gold and aluminum bonding wires used for electrical and thermal contacts. This had two consequences degrading the detector performance. One of them is that the thermal time constant of the detector was longer than expected, leading to a large fraction – more than 50% – of piled-up pulses that had to be removed from the data set. The major part of pile-up is removed by applying an extendable dead-time. A cut on the chi-square of the optimal filter used for the pulse-height determination removes practically all remaining piled-up events, too closely spaced in time to be detected separately and removed by the dead-time. The chi-square criterion is a measure for deviations of the pulse shape from the normal one. After 10 days of data acquisition at a rate of ~ 7 counts per second, the final spectrum, shown in Fig. 2, contains 2.7 million events. The other consequence is that the MMC could vibrate, resulting in an energy resolution near 200 eV (FWHM), about a factor 5 worse than expected from the absorber heat capacity. Nevertheless, the detector performance was much better than in the measurement published in [8]: The energy resolution was improved by a factor five, while the energy threshold was reduced from ~ 5 keV to ~ 700 eV. Fig. 2 shows also the theoretical spectrum calculated with the code BetaShape [9,10]. The deviation of the experimental spectrum at low energies may be attributed to the degraded detector performance.

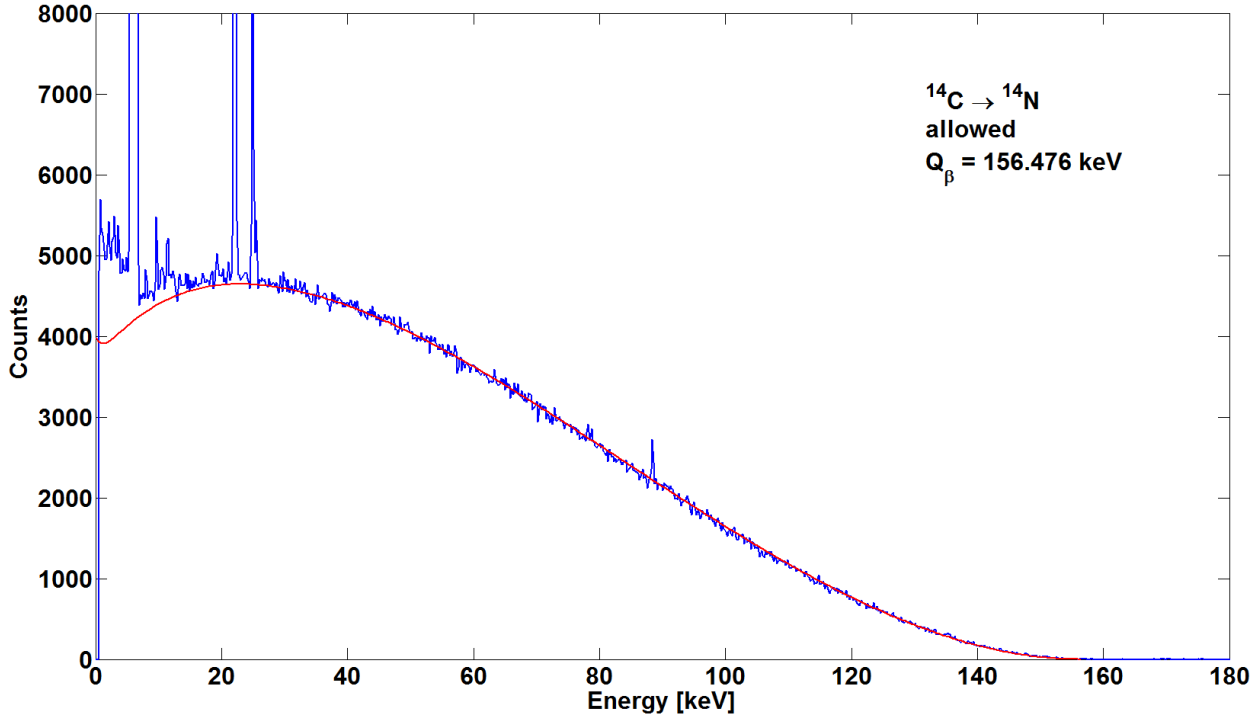

Figure 2: Beta spectrum of ^{14}C measured with an MMC (blue). The lines at 22 keV, 25 keV and 88 keV are K X-ray and gamma ray lines from an external ^{109}Cd source and the broad line at around 6 keV, in reality a clipped double line, is the Kα + β line of an external ^{55}Fe source; these lines are used for energy calibration. The weak lines at around 10 keV are escape lines. The red line is a theoretical spectrum calculated with the code BetaShape. The increase of the experimental spectrum at low energies may be due to the degraded detector performance; a new measurement under improved conditions should clarify this question.

^{151}Sm

A ^{151}Sm source was electrodeposited on a 10 µm thick silver foil. After the mechanical processing described in section 3, this source foil (0.8 mm × 0.8 mm × 7 µm) was sandwiched between two silver foils (0.9 mm × 0.9 mm × 15 µm each) and the three foils were diffusion-welded to form the absorber (heat capacity: 29 pJ/K at 20 mK). The performance of the MMC during this measurement was as expected. An energy resolution ranging from about 45 eV (FWHM) at 6 keV to 70 eV at 25 keV and an energy threshold of 250 eV were observed. It should be mentioned here that under optimal conditions the energy resolution of an MMC is nearly independent of energy since it is only limited by noise. Various effects like temperature fluctuation of the thermal bath can, however, introduce some energy-dependent terms. The thermal time constant (1/e) of the detector was 460 µs; at a count rate of 8.7 s^{-1}, the fraction of piled-up pulses was very low. After 14 days of data acquisition, the spectrum contains 10.2 million events after pile-up suppression.

^{151}Sm is the only non-pure beta emitter measured within the MetroBeta project: It has a main β^- decay branch (Q_β = 76.3 keV) to the ground state and a second β^- decay branch to the 21.54 keV excited level of ^{151}Eu. Both transitions are first forbidden non-unique. The recommended values for the respective probabilities of the two decay paths are 99.07 (4) % and 0.93 (4) % [11]. The de-excitation of the 21.54 keV excited state is highly converted; only 3.4% of the gamma transition lead to the emission of gamma-rays (total probability: 3.24 (13) × 10^{-4}), the rest leads to the emission of conversion electrons and subsequently X-rays and/or Auger electrons. The detector absorber with its given dimensions, sufficient to stop all beta electrons up to the beta *Q* value, does also stop all conversion electrons, more than 99% of all X-rays and more than 95% of the 21.54 keV gamma photons. The result is that for practically all beta decays to the excited level the sum of the beta

energy and the gamma energy is absorbed. So the measured spectrum for the decays to the excited level is shifted by the energy of the gamma transition and starts at 21.54 keV, leading to a step in the recorded spectrum. Since the maximum energy for this beta branch equals the *Q* value minus the gamma transition energy, the end point of both measured spectra is the same, 76.3 keV. As it is not possible to distinguish events from the two decay branches, both spectra are superimposed in one experimental spectrum.

The measured spectrum is shown in Fig. 3 together with theoretical spectra calculated with the code BetaShape for both decay paths. The spectrum corresponding to the decay to the ground state was fitted to the experimental spectrum in the energy range from 10 keV to 20 keV. It can clearly be seen that above 21.5 keV the experimental spectrum lies higher than the fitted spectrum of the main decay branch. The spectrum corresponding to the decay to the excited level was shifted by 21.54 keV and fitted to the experimental spectrum in the energy range 26 keV – 40 keV. The area lying between the two theoretical spectra, corresponding to the probability of the decay to the excited state of ^{151}Eu, amounts to 2.6% of the total. We do not state any uncertainty on the measured probability, firstly because the theoretical spectra are preliminary, secondly because the theoretical spectrum does not fit the experimental spectrum below 6 keV, and thirdly because the fitting procedure was rather coarse. Nevertheless, this value is in clear contradiction with the recommended value for the probability of the decay to the ^{151}Eu excited level. Concerning the beta spectrum shape, the discrepancy between experiment and theory at low energies is most likely due to an incomplete control of the atomic effects in the theoretical calculation of this first forbidden, non-unique transition.

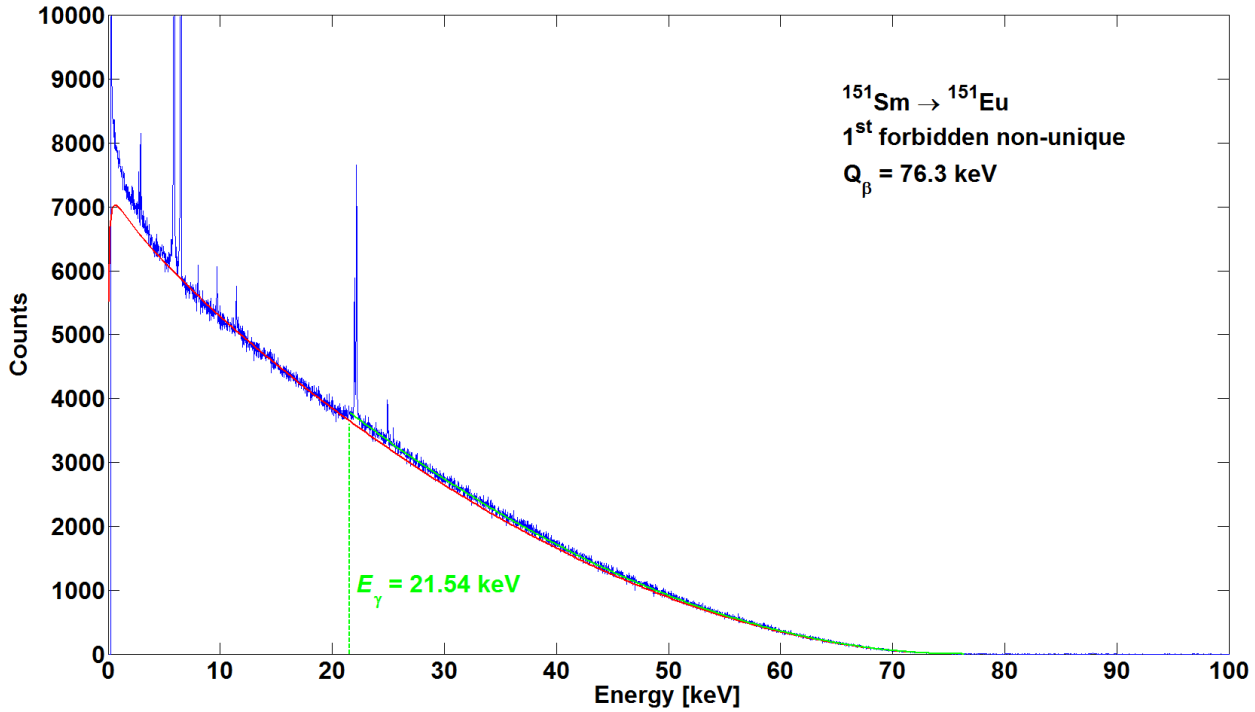

Figure 3: Beta spectrum of ^{151}Sm measured with an MMC (blue) together with theoretical spectra calculated for the two beta decay branches, to the ground state (red) and to the 21.54 keV excited level of ^{151}Eu (green). The spectrum from the transition to the excited state is shifted towards higher energies by 21.54 keV, the energy of the gamma transition that is detected in sum with the beta particle energy. Therefore both measured spectra end at the same energy, 76.3 keV. The energy calibration was performed with an external X-ray source composed of ^{55}Fe and ^{109}Cd.

^{36}Cl

A ^{36}Cl source has been fabricated by means of the micro-drop dispenser directly on a 300 µm thick gold foil formatted to an array of absorber elements with lateral dimensions of about 1.6 mm and 0.7 mm, like the one shown in Fig. 1a. An identical foil was diffusion welded onto the first foil with the dried radioactive material. One of the 1.6 mm-absorbers (heat capacity at the detector operating temperature, i. e. 20 mK: 1.8 nJ/K) was glued to one of the sensors of an XL MMC-chip, very well matched to the absorber heat capacity (optimized for 1.7 nJ/K). An external ^{241}Am source was added to the setup and the photons were collimated onto the gold absorber for energy calibration. The setup was mounted in the PTB dilution refrigerator; data was acquired at 20 mK during 140 hours. After data analysis including several cuts, the final spectrum, shown in fig. 5, contains 750000 events.

This measurement was suffering from two problems. Firstly, the pulse time constants were much longer than intended. This can be explained by the new chip design, whose behaviour was not yet well enough known at the date of the measurement, and by the heat capacity of the absorber that is extremely large for a cryogenic detector. The time constants can, however, be adjusted in a forthcoming measurement. Secondly, the vibrations of the pulse tube providing the cooling power at 3.5 K produced a parasitic signal with an amplitude several times larger than the pulse height of the beta decay events in the detector. This degraded the energy resolution to ~ 3.8 keV at the 59.54 keV ^{241}Am gamma ray line. Since this experiment the strong vibrations could be very efficiently damped at the detector level by a spring suspension of the detector support plate. This lead to a drastic improvement of the energy resolution as will be seen in the following section on the ^{99}Tc beta spectrum.

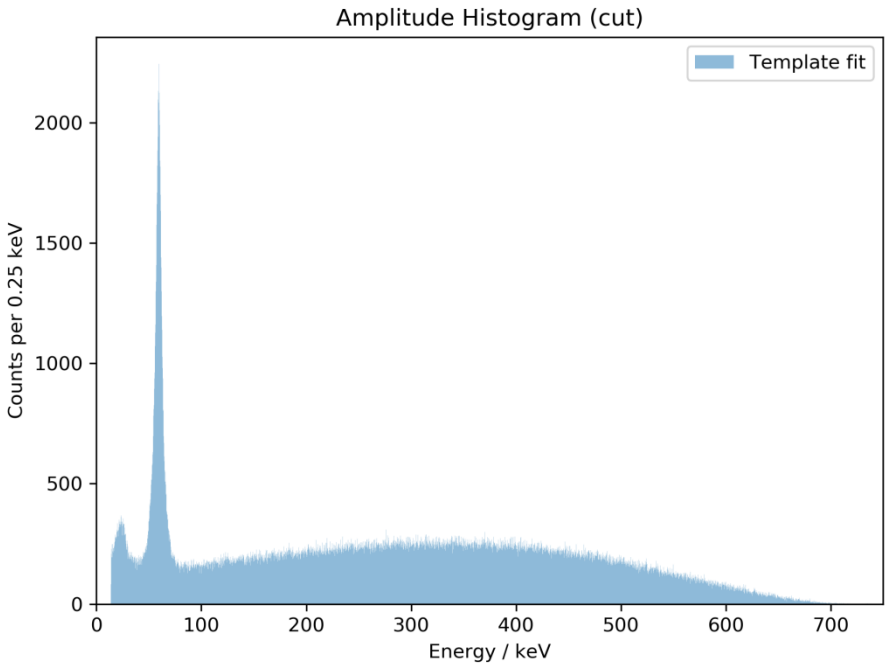

Figure 3: Beta spectrum of ^{36}Cl measured with an MMC. Energy calibration was performed using the gamma-ray photons from an external ^{241}Am source.

The theoretical calculation of this type of transition, second order forbidden non-unique, is notoriously very complex. At the state the development of the code BetaShape has reached within this project, the transition of ^{36}Cl cannot be calculated yet, although both the nuclear and atomic components alone are rather well under control. In the literature one can find several theoretical spectra for ^{36}Cl, but they are quite discrepant from one another, so to date the measured spectrum cannot be reasonably compared to a theoretical spectrum shape. However once it will be re-measured under better experimental conditions, it will be of invaluable use to constrain existing and future approaches

in the theoretical calculation. The extension of the code BetaShape for higher order, non-unique transitions is expected to be part of a follow-up project.

^{99}Tc

The beta spectrum of ^{99}Tc was measured both at PTB and at LNHB. What makes this comparison interesting is that these measurements are completely independent. The technetium sources were prepared by different techniques and are of different chemical composition. The MMCs were mounted in different detector modules. The measurements used different cryogenic setups in different electromagnetic environment. Data were recorded by different data acquisition systems, and data analysis was performed using different routines.

At LNHB, a ^{99}Tc source was electrodeposited on a 10 µm thick gold foil. The deposit is extremely thin and should be metallic technetium. However, the deposition yield and the resulting activity per surface area were lower than expected. Therefore a sufficiently large piece of this foil had to be folded three times to reduce its area to a size (~0.5 mm × 0.7 mm) small enough to enclose it in an MMC absorber. This source foil was then sandwiched between two gold foils (0.9 mm × 0.9 mm × 74 µm each) and this stack was diffusion welded. The final absorber had a heat capacity of 350 pJ/K at 20 mK, much larger than the previous detectors. The pulses had a rise time (10% - 90%) of 14 µs and a decay time (1/e) of 2.15 ms. Data was acquired during 13.7 days and the spectrum contains 5.65 million events. The energy resolution is practically energy-independent, about 100 eV (FWHM) up to 384 keV, the highest energy gamma line of a ^{133}Ba source used for energy calibration and check of the linearity. Comparing the measured and the tabulated line energies between 31 keV and 384 keV shows no larger deviations than 70 eV, less than the energy resolution, and no obvious trend.

At PTB, a ^{99}Tc source was prepared with a micro-drop dispenser directly on a 90 µm thick gold foil formatted to an array of absorber elements with lateral dimensions of about 1.6 mm and 0.7 mm, shown in Fig. 2a. An identical foil was diffusion welded onto the first foil with the dried radioactive material. One of the larger source/absorber assemblies with an expected activity of about 5 Bq was selected and glued onto a matching MMC. The heat capacity of the absorber assembly is 545 pJ/K at 20 mK. The observed pulses had a rise time (10% - 90%) of 31 µs and a decay time (1/e) of 4.6 ms. The data acquisition took 42 h and the resulting spectrum consisted of 0.5 million events with an energy threshold of about 5 keV. A ^{57}Co source was used for energy calibration and the 122 keV gamma line showed an energy resolution of 600 eV (FWHM). The larger absorber and total heat capacity of the setup, as well as experimental problems with the temperature stability of the thermal bath explain the degraded energy resolution and threshold compared to the measurement performed at LNHB.

Figure 4 shows a superposition of both experimental spectra. It is clear that the spectrum shape is practically the same. As in the case of ^{36}Cl, this spectrum shape will be a valuable input for the improvement of the theoretical calculation for this type of transition, 2nd forbidden non-unique. The theoretical spectrum that is also shown in Fig. 4 has been calculated with the current version of the code BetaShape, supposing an allowed transition, and multiplied with an experimental shape factor [12]. It is not surprising that this shape factor, derived from a measurement with an energy threshold at 55 keV, cannot correctly reproduce the spectrum at lower energies. It is noteworthy that the spectrum measured at LNHB has an energy threshold of 650 eV, practically two orders of magnitude lower than any spectrum published to date.

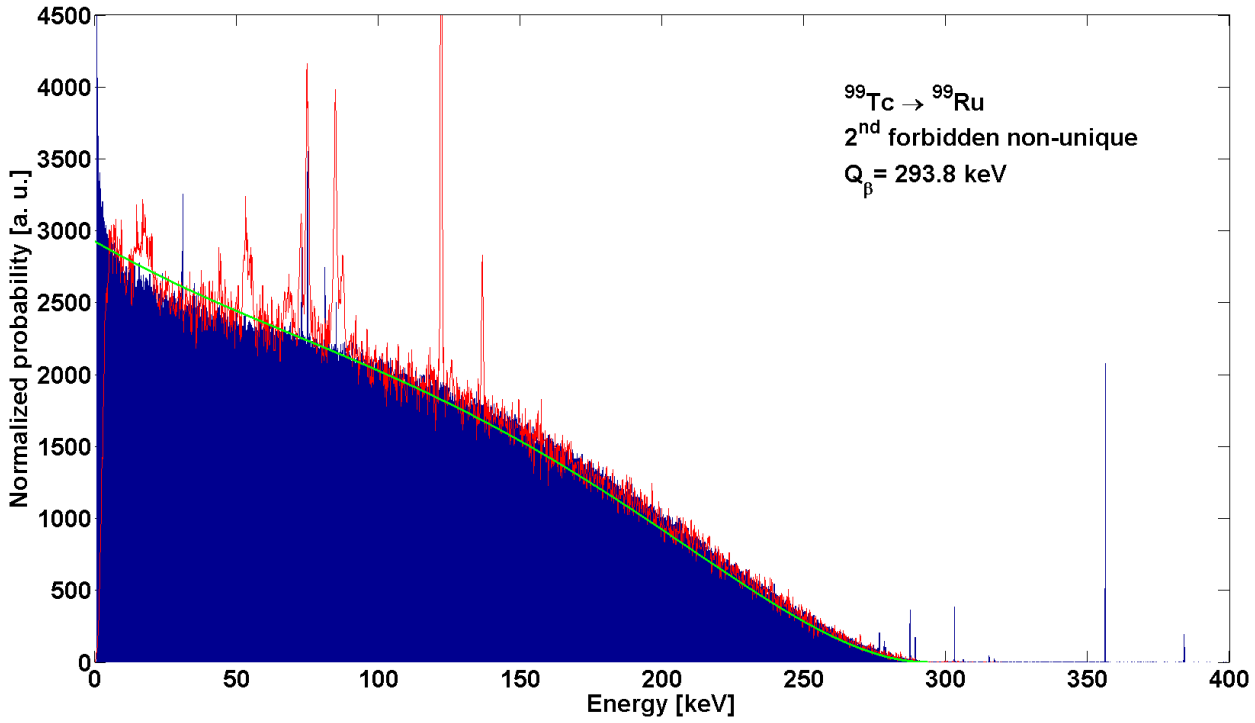

Figure 4: Beta spectrum of ^{99}Tc measured with ^{99}Tc sources fabricated in two different ways, with two independent MMCs, in different setups and using different data analysis routines. For better visibility, one spectrum is represented as a histogram (blue, measured at LNHB) and the other one as a line (red, measured at PTB). The energy calibration was performed with a ^{133}Ba source (LNHB) respectively a ^{57}Co source (PTB). A theoretical spectrum calculated with the code BetaShape is also shown (green).

3 Conclusion

Within the MetroBeta project, the beta spectra of ^{14}C, ^{36}Cl, ^{151}Sm and ^{99}Tc have been measured with the radionuclide sources enclosed in the noble metal absorbers of metallic magnetic calorimeter detectors optimized for beta spectrometry. Although in some of the measurements (^{14}C and ^{36}Cl) experimental difficulties have degraded the detector performance, the ^{151}Sm and ^{99}Tc spectra exhibit outstanding energy resolution and very low energy thersholds. The energy resolution of the ^{99}Tc spectrum, 100 eV up to 384 keV, corresponds to a resolving power of nearly 4000, one of the best reported for any energy dispersive detector. Theoretical calculations have also been performed for several nuclides; the second order forbidden, non-unique transitions of ^{36}Cl and ^{99}Tc are, however, still too complex to calculate at the state the development of the code BetaShape has reached within this project. The comparison of the experimental and theoretical spectra of ^{14}C and ^{151}Sm shows a very good overall agreement, except in the very low energy region. In the case of ^{14}C the discrepancy at low energies can be attributed to sub-optimal experimental conditions, in the case of ^{151}Sm to the incomplete control of the atomic effects at low energies in the theoretical calculation of this first forbidden, non-unique transition.

References

[1] Enss, C. Fleischmann, A., Horst, K., Schönefeld, J., Sollner, J., Adams, J. S., Huang, Y. H., Kim, Y. H. and Seidel, G., 2000. Metallic Magnetic Calorimeters for Particle Detection. J. Low Temp. Phys. 121, 137-176

[2] Fleischmann, A., Enss, C. and Seidel, G., 2005. Metallic Magnetic Calorimeters, in *Cryogenic Particle Detectors*. Topics Appl. Phys. 99, Enss, C. (Ed.), Springer Berlin/Heidelberg, 151 – 2163

[3] Loidl, M., Le-Bret, C., Rodrigues, M. and Mougeot, X., 2014. Evidence for the exchange effect down to very low energy in the beta decays of ^{63}Ni and ^{241}Pu. J. Low Temp. Phys. 176, 1040-1045

[4] Le-Bret, C., Loidl, M., Rodrigues, M., Mougeot, X., and Bouchard, J., 2012. Study of the influence of the source quality on the determination of the shape factor of beta spectra. J. Low Temp. Phys. 167, 985-990

[5] Hoover, A. S., Bond, E. M., Croce, M. P., Holesinger, T. G., Kunde, G. J., Rabin, M. W., Wolfsberg, L. E., Bennett, D. A., Hays-Wehle, J. P., Schmidt, D. R., Swetz, D. and Ullom, J. N., 2015. Measurement of the ^{240}Pu/^{240}Pu Mass Ratio Using a Transition-Edge-Sensor Microcalorimeter for Total Decay Energy Spectroscopy, Anal. Chem. 87, 3996-4000

[6] Rodrigues, M., Laarraj, M., Loidl, M., Navick, X.-F. and Mariam, R., 2018. Development of total decay energy spectrometry of α-emitting radionuclides using metallic magnetic calorimeters. J. Low Temp. Phys. 193 (2018) 1263-1268

[7] Sun Y. and Balk, T. J., 2008. A multi-step dealloying method to produce nanoporous gold with no volume change and minimal cracking. Scripta Materialia 58, 727-730

[8] Loidl, M., Beyer, J., Bockhorn, L., Enss, C., Györi, D, Kempf, S., Kossert, K., Mariam, R., Nähle, O., Paulsen, M., Rodrigues and M., Schmidt, M., 2018. MetroBeta: Beta Spectrometry with Metallic Magnetic Calorimeters in the Framework of the European Program of Ionizing Radiation Metrology. J. Low Temp. Phys. 193, 1251-1256

[9] Mougeot, X. and Bisch, C., 2014. Consistent calculation of the screening and exchange effects in allowed β^- transitions, Phys. Rev. A 90, 012501 – 1-8

[10] Mougeot, X., 2015. Reliability of usual assumptions in the calculation of β and ν spectra. Phys. Rev. C 92, 059902 and Erratum: Reliability of usual assumptions in the calculation of β and ν spectra Physical Review C 91, 055504; Erratum Phys. Rev. C 92, 059902

[11] Bé, M.-M., Chisté, V, Dulieu, C., Kellett, M. A., Mougeot, X., Arinc, A., Chechev, V. P., Kuzmenko, N. K., Kibédi, T., Luca, A. and Nichols, A. L., 2016. Table of Radionuclides, Monographie BIPM-5, vol. 8, vol. 3, ISBN-13 978-92-822-2264-5

[12] Reich, M. and Schüpferling, H.M., 1974. Formfaktor des β-Spektrums von ^{99}Tc. Z. Phys. 271, 107-113